# Strain-Rate-Dependent Mechanical Behavior of a Non-Equimolar CoCrFeMnNi High Entropy Alloy with a Segmented Coarse Grain Structure: Supplementary Document

Haoyang Li[a,*], Chenwei Shao[b], Okan K. Orhan[c], David Funes Rojas[c], Mauricio Ponga[c,**], James D. Hogan[a]

[a] *Department of Mechanical Engineering, University of Alberta, Edmonton, AB T6G 2R3, Canada*
[b] *Laboratory of Fatigue and Fracture for Materials, Institute of Metal Research, Chinese Academy of Sciences, Shenyang 110016, People's Republic of China*
[c] *Department of Mechanical Engineering, University of British Columbia Vancouver Campus, BC V6T 1Z4, Canada*

[*] Corresponding author
[**] Corresponding author
*Email addresses:* haoyang@ualberta.ca (Haoyang Li), mponga@mech.ubc.ca (Mauricio Ponga)

## Appendix A: Background and Computational Details of Gibbs Free Energy Calculations

*0.1. Background*

The Gibbs free energy for a given composition can be expressed as the following with respect to the equimolar reference case,

$$G = H^{\mathrm{mix}} + F^{\mathrm{el}} + F^{\mathrm{vib}} - TS_{\mathrm{conf}}, \tag{1}$$

where $H^{\mathrm{mix}}$, $F^{\mathrm{el}}$, $F^{\mathrm{vib}}$ and $S_{\mathrm{conf}}$ are the enthalpy of mixing, the electronic Helmholtz energy, the vibrational Helmholtz energy and the configurational entropy with respect to the equimolar CoCrFeMnNi alloy, respectively.

The enthalpy of mixing, $H^{\mathrm{mix}}$, can be approximated using the enthalpy of mixing of binary bulk metallic glasses, given by Youssef et al. [1],

$$H^{\mathrm{mix}} = \sum_{i<j} 4c_i c_j H_{ij}^{\mathrm{mix}}, \tag{2}$$

where $c_i$ is the molar fraction of the $i-$th element in the alloy and $H_{ij}^{\mathrm{mix}}$ for the relevant pairs are available within the Miedema's model in Ref. 2.

The electronic and vibrational Helmholtz free energies can be obtained using the approximate Kohn-Sham density-functional theory (KS-DFT) [3, 4] and its perturbative extension, namely the density-functional perturbation theory (DFPT) [5, 6]. The electronic component is given by [7–9],

$$\begin{aligned} F_{\mathrm{el}} = &\left( \int dE\ N(E,V) f E - \int^{E_{\mathrm{F}}} dE\ N(E,V) E \right) \\ &- T \left( -k_{\mathrm{B}} \int dE\ N(E,V) \left[ f ln(f) + (1-f) ln(1-f) \right] \right), \end{aligned} \tag{3}$$

where $k_{\mathrm{B}}$ is the Boltzmann constant; $N(E,V)$ is the electronic density of states (DOS); $f = f(E, E_{\mathrm{F}}, T)$ is the Fermi-Dirac distribution function around the Fermi level with the Fermi energy, $E_{\mathrm{F}}$. The vibrational component is given by [10, 11],

$$F_{\mathrm{vib}}(T) = k_{\mathrm{B}} T \int_0^{\infty} d\omega\ \ln \left[ 2\ \sinh \left( \frac{\hbar\omega}{2k_{\mathrm{B}}T} \right) \right] g(\omega), \tag{4}$$

where $g(\omega)$ and $k_{\mathrm{B}}$ are the phonon DOS and the Boltzmann's constant, respectively. Furthermore, the spatial disorderliness of HEAs can be expediently achieved at a disordered mean-filed limit using the virtual-crystal approximation (VCA) [12, 13] by mixing the atomic pseudo-potentials [13, 14].

Finally, the configurational entropy due to the spatial disorderliness is given within the the Stirling approximation by Santodonato et al. [15],

$$S^{M}_{\mathrm{conf}} = -R \sum_{i}^{N} c_i ln(c_i), \tag{5}$$

where $R$ is the gas constant. To assess the thermal stability of the non-equimolar mixtures, we will compare the difference in the Gibbs free energies ($\Delta G$) taking as reference the equimolar CoCrFeMnNi composition ($G_{\mathrm{ref}}$),

$$\Delta G = G - G_{\mathrm{ref}}. \tag{6}$$

*0.2. Computational Details*

The SG15 optimized norm-conserving Vanderbilt (ONCV) scalar-relativistic pseudo-potentials [16, 17] using the Perdew-Burke-Ernzerhof (PBE) exchange-correlation functional [18–20] were used for elemental atomic pseudo-potentials. A generic face-centered-cubic was used for HEAs. Variable-cell geometry optimizations were performed using the Quantum ESPRESSO (QE) software [21, 22] with a common high kinetic energy cutoff of 150 Ry, and a choice of the smearing parameter for the Marzari-Vanderbilt cold smearing [23] equivalent to 300 K at a shifted $12 \times 12 \times 12$ Monkhorst-Pack-equivalent [24] uniform Brillouin zone with a $10^{-7}$ Ry total-energy, and $10^{-6}$ Ry$\cdot$a$_0^{-1}$ total force convergence thresholds, and $10^{-10}$ self-consistency threshold. Thermal functions, elastic properties, and phonon dispersion were performed using *"thermo_pw"* package within the QE software. A uniform $4 \times 4 \times 4$ Monkhorst-Pack grid is used for phonon-dispersion simulations with a $10^{-12}$ self-consistency threshold.

**Supplementary Figures and Tables**

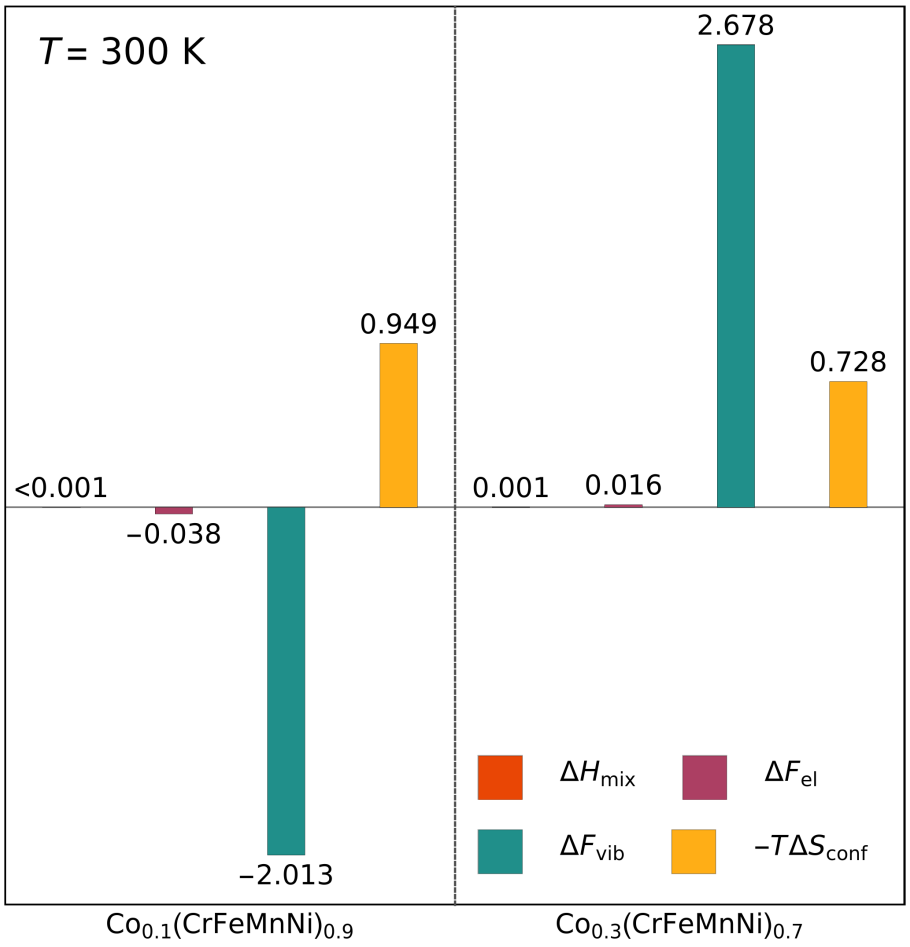


Figure 1: Individual contributions to the relative Gibbs free energy (ΔG) of the Co-reduced $Co_{0.1}(CrFeMnNi)_{0.9}$ and Co-rich $Co_{0.3}(CrFeMnNi)_{0.7}$ alloys with respect to the equimolar CoCrFeMnNi alloy. For the Co-reduced $Co_{0.1}(CrFeMnNi)_{0.9}$ case, the negative vibrational Helmholtz free energy overcomes the more positive configurational entropy, which results in a thermally more stable product.

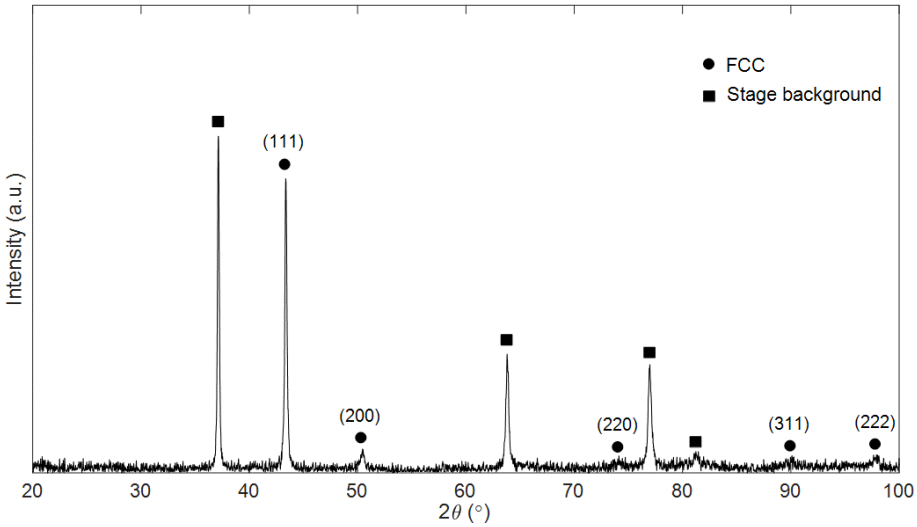


Figure 2: 1D-XRD spectrum showing single FCC phase present in the $Co_{11.3}Cr_{20.4}Fe_{22.6}Mn_{21.8}Ni_{23.9}$ (wt%) high entropy alloy. The stage background peaks are included for completeness.

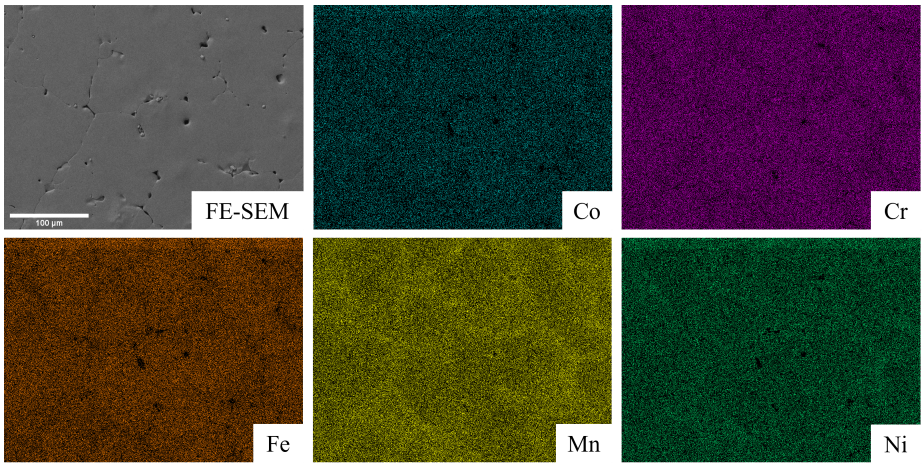


Figure 3: EDS mapping taken within a single high angle coarse grain showing thick band like features allocated at the low angle sub grain boundaries (more obvious in the Mn and Fe maps).

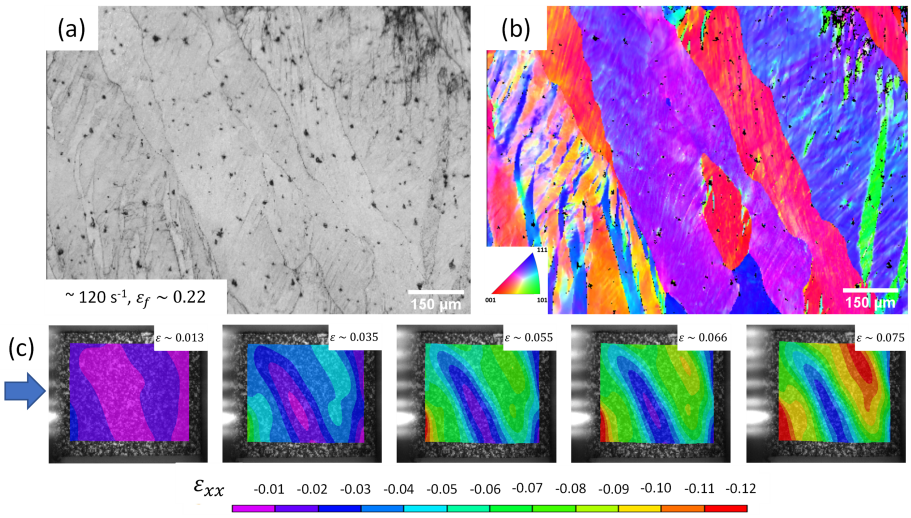


Figure 4: (a) band contrast and (b) EBSD IPF map showing the deformation features at an intermediate strain rate ($\sim$ 120 $s^{-1}$). (c) The corresponding DIC axial strain contour showing an good alignment of surface deformation bands and the grain growth direction.

Table 1: Chemical composition of the SCG-HEA confirmed by using inductively coupled plasma mass spectrometry (ICP-MS), energy dispersive spectroscopy (EDS), and x-ray photoelectron spectroscopy (XPS) methods.

| Element | ICP-MS method (wt%) | EDS method (wt%) | XPS method (wt%) |
|---|---|---|---|
| Fe | 22.66 | 22.06 | 19.27 |
| Mn | 21.82 | 22.79 | 23.96 |
| Ni | 23.80 | 22.97 | 24.37 |
| Cr | 20.41 | 20.91 | 20.13 |
| Co | 11.31 | 11.27 | 12.27 |

Table 2: Summary of the mechanical properties of the SCG-HEA alloy.

| Property | Values |
|---|---|
| Density | 7.72 $\pm$ 0.08 g/$cm^3$ |
| Yield strength | 160 - 330 MPa |
| Young's modulus | 96.2 $\pm$ 4.1 GPa |
| Poisson's ratio | 0.350 $\pm$ 0.026 |
| Microhardness | 2.84 $\pm$ 0.09 GPa |

## References


[1] K. M. Youssef, A. J. Zaddach, C. Niu, D. L. Irving, C. C. Koch, A novel low-density, high-hardness, high-entropy alloy with close-packed single-phase nanocrystalline structures, Materials Research Letters 3 (2) (2015) 95–99.

[2] A. Takeuchi, A. Inoue, Classification of bulk metallic glasses by atomic size difference, heat of mixing and period of constituent elements and its application to characterization of the main alloying element, Materials Transactions 46 (12) (2005) 2817–2829.

[3] P. Hohenberg, W. Kohn, Inhomogeneous electron gas, Physical review 136 (3B) (1964) B864.

[4] W. Kohn, L. J. Sham, Self-consistent equations including exchange and correlation effects, Physical review 140 (4A) (1965) A1133.

[5] X. Gonze, C. Lee, Dynamical matrices, born effective charges, dielectric permittivity tensors, and interatomic force constants from density-functional perturbation theory, Physical Review B 55 (16) (1997) 10355.

[6] X. Gonze, First-principles responses of solids to atomic displacements and homogeneous electric fields: Implementation of a conjugate-gradient algorithm, Physical Review B 55 (16) (1997) 10337.

[7] Y. Wang, Z.-K. Liu, L.-Q. Chen, Thermodynamic properties of al, ni, nial, and ni3al from first-principles calculations, Acta Materialia 52 (9) (2004) 2665–2671.

[8] L. Landau, E. Lifshitz, Statistical physics, v. 5, Course of Theoretical Physics 23 (1980).

[9] F. Tian, A review of solid-solution models of high-entropy alloys based on ab initio calculations, Frontiers in Materials 4 (2017) 36.

[10] A. Van De Walle, G. Ceder, The effect of lattice vibrations on substitutional alloy thermodynamics, Reviews of Modern Physics 74 (1) (2002) 11.

[11] S.-L. Shang, Y. Wang, D. Kim, Z.-K. Liu, First-principles thermodynamics from phonon and debye model: Application to ni and ni3al, Computational Materials Science 47 (4) (2010) 1040–1048.

[12] L. Nordheim, Zur elektronentheorie der metalle. i, Annalen der Physik 401 (5) (1931) 607–640.

[13] L. Bellaiche, D. Vanderbilt, Virtual crystal approximation revisited: Application to dielectric and piezoelectric properties of perovskites, Physical Review B 61 (12) (2000) 7877.

[14] V. Heine, The pseudopotential concept, Solid state physics 24 (1970) 1–36.

[15] L. J. Santodonato, Y. Zhang, M. Feygenson, C. M. Parish, M. C. Gao, R. J. Weber, J. C. Neuefeind, Z. Tang, P. K. Liaw, Deviation from high-entropy configurations in the atomic distributions of a multi-principal-element alloy, Nature communications 6 (1) (2015) 1–13.

[16] D. Hamann, Optimized norm-conserving vanderbilt pseudopotentials, Physical Review B 88 (8) (2013) 085117.

[17] M. Schlipf, F. Gygi, Optimization algorithm for the generation of oncv pseudopotentials, Computer Physics Communications 196 (2015) 36–44.

[18] D. Hamann, M. Schlüter, C. Chiang, Norm-conserving pseudopotentials, Physical Review Letters 43 (20) (1979) 1494.

[19] G. Kerker, Non-singular atomic pseudopotentials for solid state applications, Journal of Physics C: Solid State Physics 13 (9) (1980) L189.

[20] D. Hamann, Generalized norm-conserving pseudopotentials, Physical Review B 40 (5) (1989) 2980.

[21] P. Giannozzi, S. Baroni, N. Bonini, M. Calandra, R. Car, C. Cavazzoni, D. Ceresoli, G. L. Chiarotti, M. Cococcioni, I. Dabo, et al., Quantum

espresso: a modular and open-source software project for quantum simulations of materials, Journal of physics: Condensed matter 21 (39) (2009) 395502.

[22] P. Giannozzi, O. Andreussi, T. Brumme, O. Bunau, M. B. Nardelli, M. Calandra, R. Car, C. Cavazzoni, D. Ceresoli, M. Cococcioni, et al., Advanced capabilities for materials modelling with quantum espresso, Journal of physics: Condensed matter 29 (46) (2017) 465901.

[23] N. Marzari, D. Vanderbilt, A. De Vita, M. Payne, Thermal contraction and disordering of the al (110) surface, Physical review letters 82 (16) (1999) 3296.

[24] H. J. Monkhorst, J. D. Pack, Special points for brillouin-zone integrations, Physical review B 13 (12) (1976) 5188.